Biochemical and Biophysical Research Communications 453 (2014) 443–448

Contents lists available at ScienceDirect

Biochemical and Biophysical Research Communications

journal homepage: www.elsevier.com/locate/ybbrc

Restoration of cellular ubiquitin reverses impairments in neuronal development caused by disruption of the polyubiquitin gene *Ubb*

Han-Wook Ryu, Chul-Woo Park, Kwon-Yul Ryu *

Department of Life Science, University of Seoul, Seoul 130-743, Republic of Korea

ARTICLE INFO

Article history:
Received 20 September 2014
Available online 1 October 2014

Keywords:
Polyubiquitin gene
Ubiquitin
Free ubiquitin
Neuronal development
Apoptosis

ABSTRACT

Disruption of the polyubiquitin gene *Ubb* leads to hypothalamic neurodegeneration and metabolic disorders, including obesity and sleep abnormalities, in mice. However, it has yet to be determined whether or not these neural phenotypes in $Ubb^{-/-}$ mice are directly caused by cell autonomous defects in maintaining proper levels of ubiquitin (Ub). To directly demonstrate that reduced levels of Ub are sufficient to cause neuronal abnormalities, we investigated the characteristics of cultured neurons isolated from $Ubb^{-/-}$ mouse embryonic brains. We found that neuronal morphology, neurite outgrowth, and synaptic development were significantly impaired in $Ubb^{-/-}$ neurons. Furthermore, we observed the growth of astrocytes in $Ubb^{-/-}$ cell cultures despite the fact that cells were cultured under conditions promoting neuronal growth. When the reduced levels of free Ub, but not Ub conjugates, in $Ubb^{-/-}$ cells were restored to those of wild-type cells by providing exogenous Ub via lentivirus-mediated delivery, the increased apoptosis observed in $Ubb^{-/-}$ cells was almost completely abolished. Ectopic expression of Ub also improved neuronal and glial phenotypes observed in $Ubb^{-/-}$ cells. Therefore, our study suggests that Ub homeostasis, or the maintenance of cellular free Ub above certain threshold levels, is essential for proper neuronal development and survival.

1. Introduction

Ubiquitin (Ub) is well known for its diverse functions in eukaryotic cells, including targeting proteins for proteasomal degradation, regulation of signaling pathways, and receptor endocytosis [1–3]. Ubiquitination of substrates occurs via sequential actions of three enzymes E1–E3, resulting in monoubiquitination or polyubiquitination of substrates, which generate pools of Ub conjugates [4,5]. In contrast, the readily available free Ub pool comprises Ub removed from its substrates by deubiquitinating enzymes (DUBs) or synthesized *de novo* by the expression of two different classes of ubiquitin genes in mammals: monomeric Ub-ribosomal fusion genes (*Uba52* and *Uba80*) and stress-inducible polyubiquitin genes (*Ubb* and *Ubc*) [6–10].

Ub inside cells is in a dynamic equilibrium between free Ub and Ub conjugates, and the maintenance of free Ub above certain threshold levels is important for cellular function and survival, especially for neurons [11,12]. In contrast to other cell types, the availability of free Ub is a more important issue in neurons, as axonal transport of free Ub is required, but this process occurs quite slowly [13]. Therefore, limited availability of free Ub could result in uneven distribution of free Ub in different neuronal compartments and may cause severe Ub deficiency in certain compartments, such as the synapse. Ub is also known to play a crucial role during neuronal development, mostly at the level of proteasomal degradation of substrate proteins involved in neurogenesis, neuritogenesis, and synaptogenesis [14]. Timely degradation of substrates by the proteasome is also important for neuronal function and survival [15]. However, the outcome of reduced cellular Ub during neuronal development or for neuronal function has not been studied extensively.

We have previously shown that disruption of the polyubiquitin gene *Ubb* causes multiple phenotypes in mice, including infertility, hypothalamic neurodegeneration, and metabolic abnormalities [16–18]. However, it remains unknown whether or not these phenotypes are directly caused by cell autonomous defects in maintaining proper levels of Ub. In addition, it is unclear if an altered

Abbreviations: Ub, ubiquitin; DIV, days *in vitro*; TUJ1, βIII-tubulin; α-INX, α-internexin; MAP2, microtubule-associated protein 2; GFAP, glial fibrillary acidic protein; SYN1, synapsin 1; HA, hemagglutinin.

* Corresponding author at: Department of Life Science, University of Seoul, 163 Siripdae-ro, Dongdaemun-gu, Seoul 130-743, Republic of Korea. Fax: +82 2 6490 2664.

E-mail address: kyryu@uos.ac.kr (K.-Y. Ryu).

http://dx.doi.org/10.1016/j.bbrc.2014.09.103
0006-291X/

cellular and/or physiological microenvironment upon disruption of *Ubb* plays any role in causing these phenotypes in mice. Therefore, to identify the exact and direct cause of $Ubb^{-/-}$ neural phenotypes, it is essential to investigate the characteristics of cultured neurons isolated from $Ubb^{-/-}$ mouse embryonic brains.

Here, we show that neuronal morphology, neurite outgrowth, and synaptic development were significantly impaired when cellular levels of Ub were reduced by disruption of *Ubb*. To prove that the phenotypes observed upon *Ubb* disruption were direct outcomes of reduced availability of cellular Ub, we provided exogenous Ub to cells cultured *in vitro* via lentivirus-mediated delivery. As ectopic expression of Ub restored levels of free Ub in $Ubb^{-/-}$ cells and improved their phenotypes including apoptosis, our data provide direct evidence that Ub homeostasis, or the maintenance of cellular free Ub above certain threshold levels, is essential for proper neuronal development and survival.

2. Materials and methods

2.1. Isolation and culture of mixed neuronal cells

$Ubb^{+/-(eGFP\text{-}puro)}$ mice were kept in plastic cages and bred to obtain wild-type and $Ubb^{-/-}$ embryos [18]. All animal procedures were approved by the University of Seoul Institutional Animal Care and Use Committee (UOS IACUC; UOS-091201-1 and UOS-121025-2). On 14.5 days post coitum (dpc), embryonic brains were dissected and the cerebellum and meninges were removed in Hank's Balanced Salt Solution (HBSS). Processed brains were transferred to 0.05% trypsin/EDTA (Cellgro) and incubated for 30 min at 37 °C with vigorous shaking. Trypsinization was quenched by adding an equal volume of cell culture medium (DMEM supplemented with 10% fetal bovine serum [FBS], 20 mM L-glutamine, and 1% antibiotics/antimycotics [Cellgro]). After centrifugation at 1000 rpm for 5 min, the brain tissue was triturated in neuronal growth medium (Neurobasal® medium supplemented with B-27® supplement [Invitrogen], 1 × GlutaMax, 0.5 mM L-glutamine, and 1% antibiotics/antimycotics [Cellgro]) by gentle pipetting through a 1000-μl tip. Triturated tissues were strained through a 40-μm nylon mesh, and resulting cells were then cultured in the same medium on a cell culture dish coated with poly-D-lysine (MW 30000–70000; Sigma–Aldrich) and laminin (Invitrogen). One-half of the medium was changed every 3 days.

2.2. Generation of lentivirus harboring HA-Ub

The pRK5-HA-Ub-WT (wild type) vector was obtained from Addgene and a 370-bp *Cla*I/*Bam*HI fragment containing an open reading frame was inserted into the pLentiM1.4-MCMV lentiviral vector digested with *Xba*I/*Bam*HI. T4 DNA polymerase was used to fill in the incompatible ends of *Cla*I and *Xba*I sites. One day before transfection, 293T cells were plated on 100-mm dishes coated with poly-D-lysine at 2.5×10^6 cells/dish and incubated in cell culture medium (DMEM/1% FBS). To produce a lentivirus harboring HA-Ub, packaging plasmid psPAX2 (8 μg), envelope plasmid pMD2.G (3 μg), and transfer plasmid pLentiM1.4-MCMV-HA-Ub (10 μg), were mixed together in sterile buffered water (5 mM HEPES, pH 7.3) in each dish, and standard $CaPO_4$ transfection procedures were carried out. After transfection for 12 h, medium with precipitate was removed and incubated in fresh medium for another 48 h. Subsequently, the medium was collected, filtered through a 0.45-μm low-protein binding filter (Pall Corporation), mixed with Lenti-X™ concentrator according to the manufacturer's protocol (Clontech), and incubated at 4 °C overnight. After incubation, the mixture was centrifuged at 1500*g* for 45 min, and the viral pellet was resuspended in PBS, aliquoted, and stored at −80 °C.

2.3. Immunofluorescence analysis and TUNEL assay

Cells grown on poly-D-lysine-coated coverslips were fixed in 4% paraformaldehyde for 10 min at room temperature (RT), permeabilized with 0.3% Triton X-100/PBS, and blocked with 3% BSA/PBS for 1 h at RT. The fixed cells were incubated with anti-TUJ1 (1:1000, Millipore), anti-α-INX (1:1000, Millipore), anti-GFAP (1:1000, Millipore), anti-SYN1 (1:500, Millipore), anti-MAP2 (1:1000, Millipore), or anti-nestin (1:1000, Abcam) antibody at 4 °C overnight. They were then washed with PBS, and incubated with Alexa Fluor 488 or 555-conjugated goat anti-mouse or donkey anti-rabbit IgG (1:1000, Invitrogen) with 0.1 μg/ml of DAPI for 1 h at RT. Cells were then mounted using Prolong Gold antifade reagent (Invitrogen). Immunofluorescence images were visualized with a Carl Zeiss AxioImager A2 microscope or Carl Zeiss Axiovert 200 M microscope equipped with a confocal laser scanning module LSM510. Apoptotic cells were detected by TUNEL assay using an ApopTag® red *in situ* apoptosis detection kit according to the manufacturer's protocol (Millipore).

2.4. Immunoblot analysis and indirect competitive ELISA

Cell lysates were prepared in hypotonic buffer and processed as previously described [19]. Briefly, total cell lysates (15 μg) were subjected to SDS–PAGE, followed by immunoblot detection with anti-α-INX (1:3000, Millipore), anti-SYN1 (1:1000, Millipore), anti-Ub (1:1000, Enzo Life Sciences), anti-HA (1:1000, Millipore), anti-TUJ1 (1:1000, Millipore), anti-α-tubulin (1:10000, Sigma–Aldrich), or anti-β-actin antibody (1:10000, Sigma–Aldrich). Based on the types of primary antibodies, the appropriate HRP-conjugated goat anti-mouse or anti-rabbit IgG (1:10000, Enzo Life Sciences) was used. Indirect competitive ELISA was carried out as previously described [19,20].

2.5. Quantitative real-time RT-PCR

Quantitative real-time RT-PCR (qRT-PCR) was carried out as previously described with slight modifications [19]. Briefly, total RNA was isolated from cells using an RNeasy kit (Qiagen), and 10 ng of total RNA was used as a template for reverse transcription using the GoScript™ Reverse Transcription System (Promega). For qRT-PCR, we used an EvaGreen qPCR Mastermix-iCycler kit (Applied Biological Materials) and iCycler system (Bio-Rad). The mRNA expression levels of *Ubb*, *Ubc*, *Uba52*, and *Uba80* were normalized to the level of *β-actin*. Primers used for qRT-PCR are as follows: *Ubb*-F (5′-TCT GAG GGG TGG CTA TTA A-3′); *Ubb*-R (5′-TGC TTA CCA TGC AAC AAA AC-3′); *Ubc*-F (5′-GTT ACC ACC AAG AAG GTC-3′); *Ubc*-R (5′-GGG AAT GCA AGA ACT TTA TTC-3′); *Uba52*-F (5′-GTC AGC TTG CCC AGA AGT AC-3′); *Uba52*-R (5′-ACT TCT TCT TGC GGC AGT TG-3′); *Uba80*-F (5′-TGG CAA AAT TAG CCG ACT TCG-3′); *Uba80*-R (5′-AAC ACT TGC CAC AGT AAT GCC-3′); *β-actin*-F (5′-AGA GGG AAA TCG TGC GTG AC-3′); *β-actin*-R (5′-CAA TAG TGA TGA CCT GGC CGT-3′).

2.6. Statistical analysis

Two-tailed unpaired Student's *t*-test or two-way analysis of variance (ANOVA) with the Holm-Sidak method were used to compare the data between experimental and control groups. $P < 0.05$ was considered statistically significant.

3. Results and discussion

3.1. Defective neuronal development in $Ubb^{-/-}$ cells cultured in vitro

Cells isolated from midgestation mouse embryonic brains were cultured in neuronal growth medium. Although wild-type cells exhibited characteristics of neurons, $Ubb^{-/-}$ cells displayed abnormal phenotypes during culture *in vitro*. Immunofluorescence analysis using various neuronal markers such as βIII-tubulin (TUJ1), α-internexin (α-INX), and microtubule-associated protein 2 (MAP2) showed that neuronal processes in $Ubb^{-/-}$ neurons were far less complex than those in wild-type neurons, regardless of the culture period (Fig. 1A and B). From DIV7 to DIV13, wild-type neurons exhibited a more complex and extended neuritic network resembling a mature and differentiated neuronal cell phenotype, whereas $Ubb^{-/-}$ neurons displayed relatively short neurites and poor branching (Fig. 1A). These results suggest that neuronal morphology, neurite outgrowth, and axonal development were significantly impaired in $Ubb^{-/-}$ neurons. Furthermore, $Ubb^{-/-}$ neuronal cell bodies were sometimes surrounded by astrocytes that were positive for glial fibrillary acidic protein (GFAP) (Fig. 1B, left panels). Therefore, it is highly likely that neuronal development or maturation is significantly impaired by the disruption of *Ubb*.

Furthermore, immunoblot analysis showed that levels of the early neuronal marker α-INX were maintained even on DIV13 in $Ubb^{-/-}$ cells (Fig. 1C). This result is quite surprising since intact α-INX levels supposedly decrease in neurons during maturation or development [21], as observed in wild-type cells (Fig. 1C). This unexpected maintenance of α-INX levels in $Ubb^{-/-}$ cells could presumably be attributed to defective neuronal maturation or development. Interestingly, the degradation product of α-INX observed in $Ubb^{-/-}$ cells was less than that in wild-type cells during the culture period, suggesting that degradation rate of α-INX may also be affected in $Ubb^{-/-}$ cells.

In accordance with impaired neuronal development, immunoreactivity for the presynaptic marker synapsin 1 (SYN1) was also reduced in late-stage $Ubb^{-/-}$ neurons on DIV21 (Fig. 1B, right panels). Close examination of late-stage neurons revealed that the number of $SYN1^{+}$ puncta significantly decreased in $Ubb^{-/-}$ neurons (Fig. 1B, right panels). Furthermore, SYN1 protein levels were dramatically reduced in $Ubb^{-/-}$ cells cultured for 11 days or longer (Fig. 1D). As SYN1 is a synaptic vesicle-associated protein present in the axon terminal to regulate synapse formation, reduced SYN1 levels may also affect synaptic development in $Ubb^{-/-}$ neurons.

3.2. Reduced Ub levels and altered Ub pools in $Ubb^{-/-}$ cells cultured in vitro

To determine whether or not abnormalities in $Ubb^{-/-}$ neurons are the direct outcome of altered Ub pools, we first measured total Ub levels in cultured cells by indirect competitive ELISA [20]. Total Ub levels were significantly reduced in $Ubb^{-/-}$ cells throughout the culture period (Fig. 2A). This decrease in total Ub levels in $Ubb^{-/-}$ cells was due mostly to the reduction of Ub conjugates, and to a lesser extent to the reduction of free Ub (Fig. 2B). In fact, *Ubb* expression made the most significant contribution to total Ub

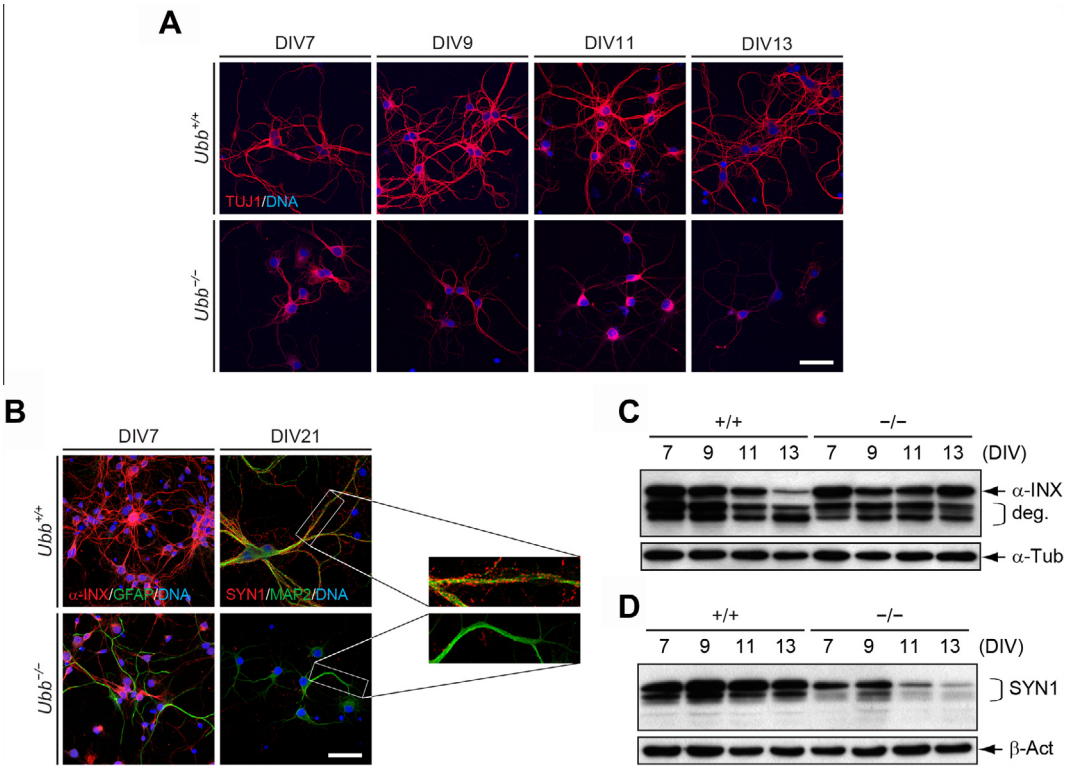

Fig. 1. Impaired neuronal development in $Ubb^{-/-}$ cells cultured *in vitro*. (A) Wild-type ($Ubb^{+/+}$) and $Ubb^{-/-}$ cells cultured *in vitro* for 7–13 days (DIV7 to DIV13) were stained with the neuronal marker TUJ1, and DNA was visualized with DAPI. (B) Wild-type ($Ubb^{+/+}$) and $Ubb^{-/-}$ cells cultured *in vitro* for 7 days (DIV7) were stained with the early neuronal marker α-INX and the glial cell marker GFAP, and DNA was visualized with DAPI. Cells cultured *in vitro* for 21 days (DIV21) were stained with the presynaptic marker SYN1 and the neuronal marker MAP2. (C and D) Immunoblot detection of α-INX and SYN1 in wild-type (+/+) and $Ubb^{-/-}$ cells (−/−) cultured *in vitro* for 7–13 days (DIV7 to DIV13). α-Tubulin (α-Tub) or β-actin (β-Act) was used as a loading control. In (C), an α-INX-immunoreactive band was detected at 66 kDa and the degradation product of α-INX was observed (deg.). In (D), SYN1-immunoreactive bands were detected at 80 and 77 kDa, representing isoforms of SYN1, synapsin 1a (SYN1a) and synapsin 1b (SYN1b). All data are representative confocal images (A and B) or representative immunoblot results (C and D) of cells from three different embryonic brains per genotype. Scale bars, 50 μm.

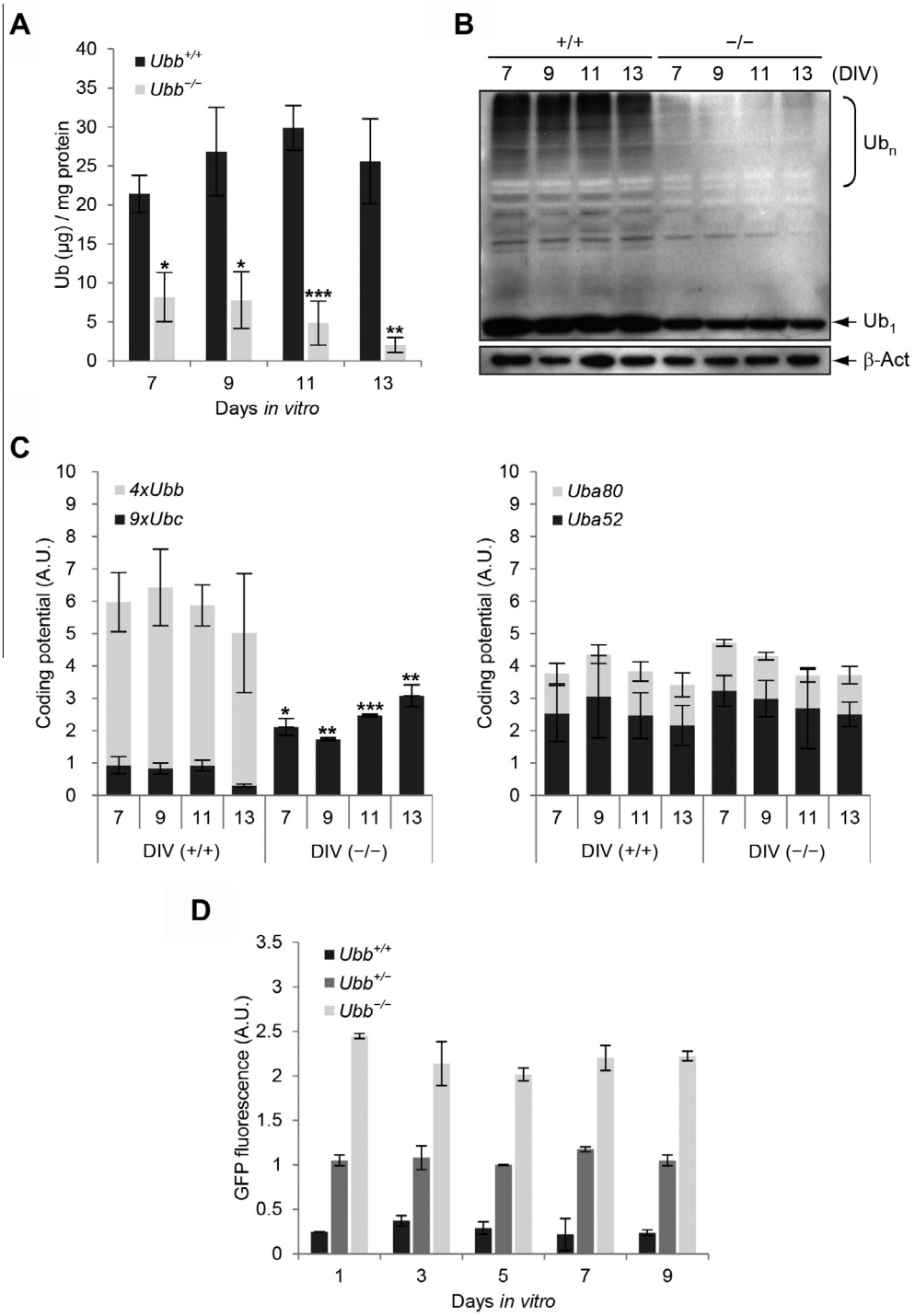

Fig. 2. Reduced Ub levels and altered Ub pools in $Ubb^{-/-}$ cells cultured *in vitro*. (A) Total Ub levels in wild-type ($Ubb^{+/+}$) and $Ubb^{-/-}$ cells ($n = 4$ each) cultured *in vitro* for 7–13 days (DIV7 to DIV13) were determined by indirect competitive ELISA. (B) Immunoblot detection of Ub conjugates (Ub_n) and free Ub (Ub_1) in wild-type (+/+) and $Ubb^{-/-}$ cells (−/−) cultured *in vitro* for 7–13 days (DIV7 to DIV13). β-Actin (β-Act) was used as a loading control. Representative immunoblot results of cells from three different embryonic brains per genotype are shown. (C) Ubiquitin mRNA levels in wild-type (+/+) and $Ubb^{-/-}$ cells (−/−) ($n = 3$ each) cultured *in vitro* for 7–13 days (DIV7 to DIV13) were determined by qRT-PCR and normalized to *β-actin* levels. Coding potential, which accounts for the relative contribution of each ubiquitin gene toward the total Ub level, was calculated by multiplying the number of Ub moieties that each ubiquitin transcript generates. (D) GFP fluorescence of wild-type ($Ubb^{+/+}$), $Ubb^{+/-}$, and $Ubb^{-/-}$ cells ($n = 2$ each) cultured *in vitro* for 1–9 days (DIV1 to DIV9) on a 96-well plate was monitored using a fluorescence plate reader. All data are expressed as the means ± SEM from the indicated number of samples. $^{*}P < 0.05$; $^{**}P < 0.01$; $^{***}P < 0.001$ *vs.* $Ubb^{+/+}$ on each day (A) or coding potential of *Ubc* in wild-type (+/+) cells (C).

levels in wild-type cells, as noted by the coding potential of *Ubb* (Fig. 2C, left). Due to the high coding potential of *Ubb* in wild-type cells, upregulation of the polyubiquitin gene *Ubc* was not sufficient to compensate for the loss of *Ubb* expression in $Ubb^{-/-}$ cells (Fig. 2C, left). On the other hand, upregulation of *Uba52* or *Uba80* was not observed in $Ubb^{-/-}$ cells (Fig. 2C, right). These results suggest that the slight upregulation of *Ubc* in $Ubb^{-/-}$ cells was not sufficient to compensate for the reduction in cellular Ub levels.

In our study, cells were cultured under conditions that promote neuronal growth. While the cultured wild-type cells were mostly neurons, $Ubb^{-/-}$ cells were composed of both neurons and astrocytes. Therefore, we investigated whether the upregulation of

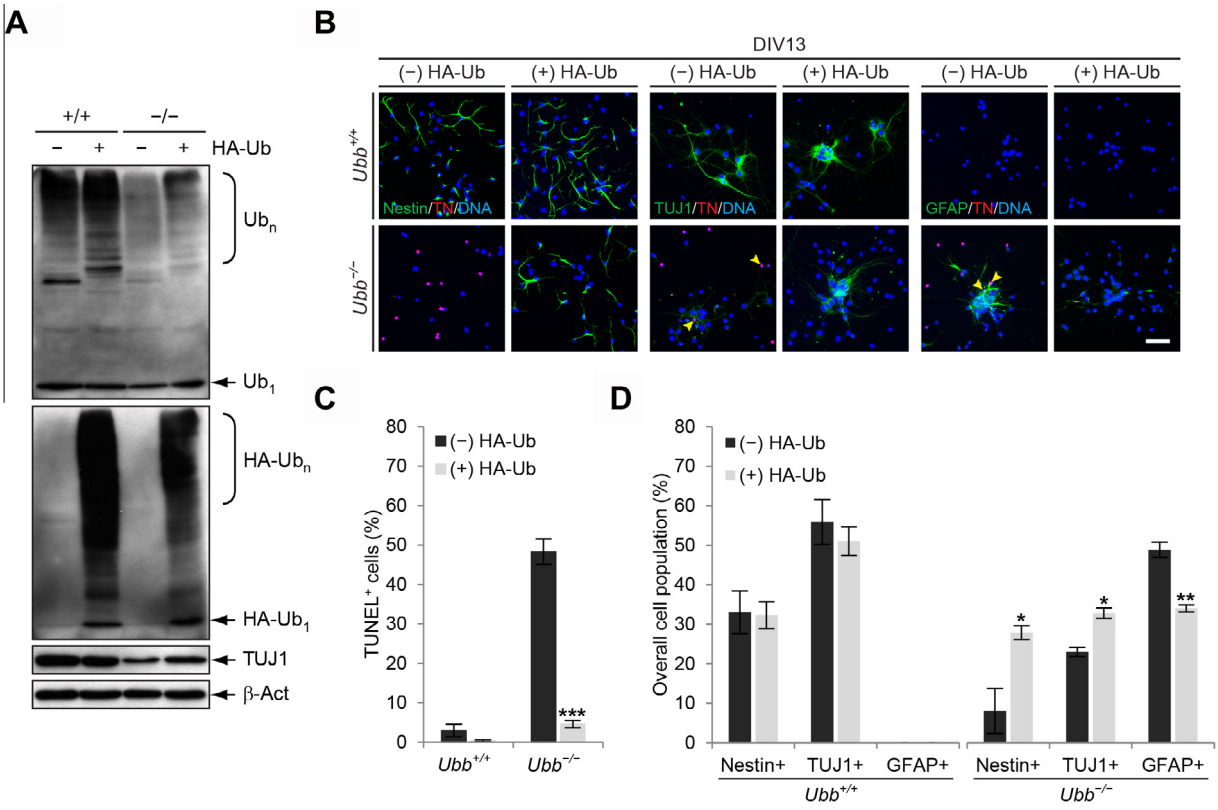

Fig. 3. Improvement of *Ubb*$^{-/-}$ neuronal and glial phenotypes with extra Ub via lentivirus-mediated delivery. (A) Wild-type (*Ubb*$^{+/+}$) and *Ubb*$^{-/-}$ cells were infected with lentivirus harboring HA-Ub (+HA-Ub) or an empty lentiviral vector (−HA-Ub) on day 1 (DIV1) and cultured *in vitro* for another 12 days (DIV13). Ub conjugates (Ub$_n$) and free Ub (Ub$_1$) levels in wild-type (+/+) and *Ubb*$^{-/-}$ cells (−/−) were determined by immunoblot analysis using an anti-Ub antibody. Expression of HA-Ub was confirmed by detecting HA-Ub conjugates (HA-Ub$_n$) and free HA-Ub (HA-Ub$_1$) using an anti-HA antibody only in cells infected with lentivirus harboring HA-Ub (+HA-Ub). TUJ1 levels were also determined, and β-actin (β-Act) was used as a loading control. (B) Wild-type (*Ubb*$^{+/+}$) and *Ubb*$^{-/-}$ cells were infected with lentivirus and cultured as described in (A). On DIV13, cells were subjected to a double-labeling fluorescence TUNEL assay (TN) with the neural stem/progenitor cell marker nestin, neuronal marker TUJ1, or glial cell marker GFAP, and DNA was visualized with DAPI. Arrowheads indicate TUNEL$^+$ (TN) apoptotic cells that are also positive for cell-type specific markers. (C) On DIV13, the percentages of apoptotic wild-type (*Ubb*$^{+/+}$) and *Ubb*$^{-/-}$ cells (n = 3 each) infected with lentivirus harboring HA-Ub ((+) HA-Ub) or an empty lentiviral vector ((−) HA-Ub) were determined. To determine the percentages of cells undergoing apoptosis, the total number of TUNEL$^+$ cells was divided by the total number of DAPI$^+$ cells in three randomly selected fields for each sample. For each sample, more than 100 DAPI$^+$ cells were counted. (D) On DIV13, the percentages of wild-type (*Ubb*$^{+/+}$) and *Ubb*$^{-/-}$ cells (n = 3 each) positive for nestin, TUJ1, or GFAP with ((+) HA-Ub) or without extra Ub ((−) HA-Ub) were determined in a similar manner as described in (C). Representative immunoblot results or images of cells from three different embryonic brains per genotype are shown (A and B), and data are expressed as the means ± SEM from the indicated number of samples (C and D). $^*P < 0.05$; $^{**}P < 0.01$; $^{***}P < 0.001$ vs. (−) HA-Ub. Scale bar, 50 μm.

Ubc in *Ubb*$^{-/-}$ cells occurred in neurons, astrocytes, or both. Based on a published transcriptome database [22], *Ubc* is upregulated in both *Ubb*$^{-/-}$ neurons and astrocytes. Although Affymetrix array data using probe sets for *Ubb* should be interpreted cautiously due to their cross-reactivity with *Ubc* and *Uba52* [23], the transcriptome database for neurons, astrocytes, and oligodendrocytes isolated from mouse brains from postnatal day 7 (P7) to P17 revealed that ubiquitin gene expression levels were comparable among various cell types [22]. These data suggest that *Ubc* slightly compensates for disruption of *Ubb*, regardless of cell type.

By monitoring GFP fluorescence from a GFP-puro^r fusion protein knocked in to the *Ubb* locus [17], we also determined *Ubb* transcriptional activity in *Ubb*$^{+/-(eGFP\text{-}puro)}$ (or simply *Ubb*$^{+/-}$) cells during the culture period. *Ubb* transcriptional activity, based on GFP fluorescence, did not change during the culture period (Fig. 2D). This result was supported by the observation that the *Ubb* coding potential remained steady during culture (see Fig. 2C, left). Due to the gene-dosage effect, GFP fluorescence in *Ubb*$^{-/-}$ cells was about twice that observed in *Ubb*$^{+/-}$ cells.

3.3. Providing exogenous Ub via lentivirus-mediated delivery to *Ubb*$^{-/-}$ cells cultured in vitro

To determine whether or not the phenotypes observed in *Ubb*$^{-/-}$ cells are simply due to reduced Ub levels upon disruption of *Ubb*, Ub levels in *Ubb*$^{-/-}$ cells were increased by ectopic expression of Ub. To accomplish this, we generated a lentivirus harboring hemagglutinin-derived epitope tagged (HA)-Ub for efficient transduction of non-dividing post-mitotic neurons as well as to distinguish it from endogenous Ub. Ub conjugates were slightly upregulated in infected *Ubb*$^{-/-}$ cells, whereas levels of free Ub increased to those of wild-type cells (Fig. 3A). Furthermore, HA-Ub contributed to the upregulation of Ub conjugates and free Ub (Fig. 3A). Although levels of Ub conjugates were only partially restored in infected *Ubb*$^{-/-}$ cells, restored levels of free Ub were sufficient to abolish the increased apoptosis in *Ubb*$^{-/-}$ cells (Fig. 3B and C).

Ubb$^{-/-}$ cells spared from apoptosis in the presence of extra Ub included neurons, as exogenous expression of HA-Ub increased TUJ1 immunoreactivity (Fig. 3A) and rendered apoptotic TUJ1$^+$ cells hardly detectable (Fig. 3B, middle panels). Ectopic expression of HA-Ub in *Ubb*$^{-/-}$ cells also resulted in the disappearance of apoptotic GFAP$^+$ cells (Fig. 3B, right panels). Although nestin is highly expressed in neural stem/progenitor cells, it can also be detected at early stage in differentiated neurons, as evidenced by the morphology of nestin$^+$ cells on DIV13 (Fig. 3B, left panels). Most strikingly, nestin$^+$ cells were completely absent in apoptotic *Ubb*$^{-/-}$ cells on DIV13 in contrast to wild-type cells, which frequently displayed clusters of nestin$^+$ cells. On the other hand, nestin$^+$ cells were observed in *Ubb*$^{-/-}$ cells on DIV13 in the presence of extra Ub (Fig. 3B, left panels). This result suggests that neural stem/

progenitor cells and/or early-stage neurons underwent apoptosis upon disruption of *Ubb* in the absence of extra Ub, and that these apoptotic cells could have already lost the expression of nestin (Fig. 3B, left panels).

Intriguingly, on DIV13, wild-type cells mostly comprised TUJ1$^+$ neurons (>50%), with fewer nestin$^+$ cells (~30%) (Fig. 3D, left). However, *Ubb*$^{-/-}$ cells mostly composed GFAP$^+$ astrocytes (~50%), with fewer TUJ1$^+$ (~20%) and nestin$^+$ cells (<10%) (Fig. 3D, right). By providing exogenous Ub to *Ubb*$^{-/-}$ cells, firstly, the number of nestin$^+$ cells increased dramatically (~30%), reaching wild-type levels (Fig. 3D, right). Secondly, the number of TUJ1$^+$ cells also increased (~30%), although it did not reach wild-type levels. Lastly, the number of GFAP$^+$ cells significantly decreased (~30%). Therefore, the phenotypes in *Ubb*$^{-/-}$ cells clearly improved in the presence of extra Ub.

Although further investigation is required, lentivirus-mediated delivery of exogenous Ub was sufficient to increase cellular free Ub above threshold levels, resulting in decreased apoptosis in all cell types investigated and the restoration of neuronal development in *Ubb*$^{-/-}$ cells cultured *in vitro*. These results suggest that Ub plays an important role in protecting not only neurons, but also other cell types, from degeneration or cell death. However, the partial improvement in the neuronal and glial phenotypes in *Ubb*$^{-/-}$ cells with extra Ub suggests that defects may occur even before the start of *in vitro* culture. Therefore, providing exogenous Ub at the beginning of culture on DIV1 may only improve the abnormalities that occur during the culture period. Nonetheless, our study using cells isolated from midgestation mouse embryonic brains clearly demonstrates that Ub homeostasis, or the maintenance of cellular free Ub above certain threshold levels, is essential for proper neuronal development and survival.

Acknowledgment

This study was supported by a grant from the Korean Health Technology R&D Project, Ministry of Health & Welfare, Republic of Korea (A111485) to K.-Y.R.

References

[1] A. Hershko, A. Ciechanover, The ubiquitin system, Annu. Rev. Biochem. 67 (1998) 425–479.
[2] M. Hochstrasser, Ubiquitin-dependent protein degradation, Annu. Rev. Genet. 30 (1996) 405–439.
[3] T. Ravid, M. Hochstrasser, Diversity of degradation signals in the ubiquitin-proteasome system, Nat. Rev. Mol. Cell Biol. 9 (2008) 679–690.
[4] L. Hicke, Protein regulation by monoubiquitin, Nat. Rev. Mol. Cell Biol. 2 (2001) 195–201.
[5] C.M. Pickart, D. Fushman, Polyubiquitin chains: polymeric protein signals, Curr. Opin. Chem. Biol. 8 (2004) 610–616.
[6] A.Y. Amerik, M. Hochstrasser, Mechanism and function of deubiquitinating enzymes, Biochim. Biophys. Acta 1695 (2004) 189–207.
[7] R.T. Baker, P.G. Board, The human ubiquitin-52 amino acid fusion protein gene shares several structural features with mammalian ribosomal protein genes, Nucleic Acids Res. 19 (1991) 1035–1040.
[8] D. Komander, M.J. Clague, S. Urbe, Breaking the chains: structure and function of the deubiquitinases, Nat. Rev. Mol. Cell Biol. 10 (2009) 550–563.
[9] K.L. Redman, M. Rechsteiner, Identification of the long ubiquitin extension as ribosomal protein S27a, Nature 338 (1989) 438–440.
[10] O. Wiborg, M.S. Pedersen, A. Wind, L.E. Berglund, K.A. Marcker, J. Vuust, The human ubiquitin multigene family: some genes contain multiple directly repeated ubiquitin coding sequences, EMBO J. 4 (1985) 755–759.
[11] J. Hallengren, P.C. Chen, S.M. Wilson, Neuronal ubiquitin homeostasis, Cell Biochem. Biophys. 67 (2013) 67–73.
[12] C.W. Park, K.Y. Ryu, Cellular ubiquitin pool dynamics and homeostasis, BMB Rep. 47 (2014) 475–482.
[13] A. Bizzi, B. Schaetzle, A. Patton, P. Gambetti, L. Autilio-Gambetti, Axonal transport of two major components of the ubiquitin system: free ubiquitin and ubiquitin carboxyl-terminal hydrolase PGP 9.5, Brain Res. 548 (1991) 292–299.
[14] H. Kawabe, N. Brose, The role of ubiquitylation in nerve cell development, Nat. Rev. Neurosci. 12 (2011) 251–268.
[15] H.C. Tai, E.M. Schuman, Ubiquitin, the proteasome and protein degradation in neuronal function and dysfunction, Nat. Rev. Neurosci. 9 (2008) 826–838.
[16] K.Y. Ryu, N. Fujiki, M. Kazantzis, J.C. Garza, D.M. Bouley, A. Stahl, X.Y. Lu, S. Nishino, R.R. Kopito, Loss of polyubiquitin gene Ubb leads to metabolic and sleep abnormalities in mice, Neuropathol. Appl. Neurobiol. 36 (2010) 285–299.
[17] K.Y. Ryu, J.C. Garza, X.Y. Lu, G.S. Barsh, R.R. Kopito, Hypothalamic neurodegeneration and adult-onset obesity in mice lacking the Ubb polyubiquitin gene, Proc. Natl. Acad. Sci. U.S.A. 105 (2008) 4016–4021.
[18] K.Y. Ryu, S.A. Sinnar, L.G. Reinholdt, S. Vaccari, S. Hall, M.A. Garcia, T.S. Zaitseva, D.M. Bouley, K. Boekelheide, M.A. Handel, M. Conti, R.R. Kopito, The mouse polyubiquitin gene Ubb is essential for meiotic progression, Mol. Cell. Biol. 28 (2008) 1136–1146.
[19] K.Y. Ryu, R. Maehr, C.A. Gilchrist, M.A. Long, D.M. Bouley, B. Mueller, H.L. Ploegh, R.R. Kopito, The mouse polyubiquitin gene UbC is essential for fetal liver development, cell-cycle progression and stress tolerance, EMBO J. 26 (2007) 2693–2706.
[20] K.Y. Ryu, R.T. Baker, R.R. Kopito, Ubiquitin-specific protease 2 as a tool for quantification of total ubiquitin levels in biological specimens, Anal. Biochem. 353 (2006) 153–155.
[21] M.P. Kaplan, S.S. Chin, K.H. Fliegner, R.K. Liem, Alpha-internexin, a novel neuronal intermediate filament protein, precedes the low molecular weight neurofilament protein (NF-L) in the developing rat brain, J. Neurosci. 10 (1990) 2735–2748.
[22] J.D. Cahoy, B. Emery, A. Kaushal, L.C. Foo, J.L. Zamanian, K.S. Christopherson, Y. Xing, J.L. Lubischer, P.A. Krieg, S.A. Krupenko, W.J. Thompson, B.A. Barres, A transcriptome database for astrocytes, neurons, and oligodendrocytes: a new resource for understanding brain development and function, J. Neurosci. 28 (2008) 264–278.
[23] S.A. Sinnar, C.L. Small, R.M. Evanoff, L.G. Reinholdt, M.D. Griswold, R.R. Kopito, K.Y. Ryu, Altered testicular gene expression patterns in mice lacking the polyubiquitin gene Ubb, Mol. Reprod. Dev. 78 (2011) 415–425.